

# Choroidal Structural Changes in Myopic Choroidal Neovascularization After Treatment With Antivascular Endothelial Growth Factor Over 1 Year

Wei Yan Ng,<sup>1</sup> Daniel Shu Wei Ting,<sup>1</sup> Rupesh Agrawal,<sup>2,3</sup> Neha Khandelwal,<sup>3</sup> Hla Myint Htoon,<sup>2,4</sup> Shu Yen Lee,<sup>1,4</sup> Tien Yin Wong,<sup>1,2,4,5</sup> and Gemmy Chui Ming Cheung<sup>1,2,4,5</sup>

<sup>1</sup>Singapore National Eye Centre, Singapore

<sup>2</sup>Singapore Eye Research Institute, Singapore

<sup>3</sup>National Healthcare Group Eye Institute, Tan Tock Seng Hospital, Singapore

<sup>4</sup>Ophthalmology Academic Clinical Program, Duke-NUS Medical School, Singapore

<sup>5</sup>Department of Ophthalmology, Yong Loo Lin School of Medicine, National University of Singapore, Singapore

Correspondence: Gemmy Chui Ming Cheung, Singapore Eye Research Institute, Singapore National Eye Centre, 11 Third Hospital Avenue, Singapore 168751; gemmy.cheung.c.m@sneec.com.sg.

Submitted: June 25, 2016

Accepted: August 5, 2016

Citation: Ng WY, Ting DSW, Agrawal R, et al. Choroidal structural changes in myopic choroidal neovascularization after treatment with antivascular endothelial growth factor over 1 year. *Invest Ophthalmol Vis Sci*. 2016;57:4933–4939. DOI:10.1167/iov.16-20191

**PURPOSE.** To evaluate choroidal structural changes in eyes with myopic choroidal neovascularization (mCNV) treated with anti-VEGF over 12 months.

**METHODS.** We prospectively evaluated subfoveal choroidal thickness (SFCT) and choroidal vascularity index (CVI) using spectral-domain optical coherence tomography (SD-OCT) at baseline, 6, and 12 months in both eyes in patients presenting with unilateral mCNV. Choroidal vascularity index was defined as the ratio of luminal area to total choroidal area after SD-OCT images were binarized digitally.

**RESULTS.** We included 20 patients (20 eyes with mCNV and 20 fellow eyes without mCNV) with mean age of  $60.35 \pm 10.85$  years. At baseline, mean SFCT and CVI was similar between eyes with mCNV and fellow eyes ( $69.20 \pm 63.04 \mu\text{m}$  vs.  $67.10 \pm 65.74 \mu\text{m}$ ,  $P = 0.713$  for SFCT and  $59.44 \pm 3.92\%$  vs.  $59.03 \pm 5.58\%$ ,  $P = 0.958$  for CVI). Subfoveal choroidal thickness decreased significantly in the mCNV eyes to  $54.75 \pm 45.43 \mu\text{m}$  ( $P = 0.017$ ) at 12 months after anti-VEGF therapy, whereas SFCT in the contralateral eyes did not change significantly. There was no significant change in CVI in mCNV eyes or contralateral eyes from baseline to 12 months. Thinning of SFCT did not influence final BCVA.

**CONCLUSIONS.** Thinning of subfoveal choroid without alteration in CVI was observed in eyes with mCNV treated with anti-VEGF therapy over 12 months. This finding may be explained by mechanical stretching in response to globe expansion.

**Keywords:** choroidal thickness, myopic choroidal neovascularization (mCNV), choroidal vascularity index (CVI)

Choroidal neovascularization (CNV) is a major sight-threatening complication of pathologic myopia and has a poor prognosis without treatment.<sup>1,2</sup> A reduction in choroidal circulation flow has been shown to occur in high myopia, and may be important in the pathogenesis of myopic CNV (mCNV).<sup>3</sup> Recently, a reduction in choroidal thickness (CT) in eyes with pathological myopia and mCNV has been demonstrated using OCT imaging.<sup>4–7</sup> As anti-VEGF is now the treatment of choice of myopic CNV,<sup>8,9</sup> concerns have been raised as to whether progressive thinning of choroid may develop and lead to long-term visual impairment.<sup>10</sup>

There have been few studies describing temporal changes in CT and structure in eyes with mCNV treated with anti-VEGF therapy<sup>10,11</sup> and no studies on changes in choroidal vascularity. Choroidal vascularity can now be indirectly measured using a novel technique to derive the choroidal vascular index (CVI). After binarization of the spectral-domain optical coherence tomography (SD-OCT) images, the total choroidal area (TCA) as well as vascular luminal areas (LA) are identified and measured. The objective quantitative parameter CVI is subsequently computed by dividing the LA by TCA. In a separate study of

healthy individuals by our group, we found that CVI, with reduced variability compared with choroidal thickness measurements, provided a better representation of the choroidal structure.<sup>12</sup> As the choroid is highly vascularized, ability to objectively compare the changes of the choroidal vasculature is crucial to our understanding of choroidal structural changes with CNV.

In this study, we aimed to describe longitudinal changes in the CT and choroidal vasculature in patients with myopic CNV and their fellow eyes, and to determine whether anti-VEGF therapy has any differential impact on the choroidal vasculature.

## METHODS

### Study Population

We conducted a prospective observational study of patients with pathological myopia in both eyes with newly diagnosed mCNV in one eye. This study was performed in accordance with the tenets of the Declaration of Helsinki and was approved



by the SingHealth Centralised institutional review board (Singapore). Informed consent was obtained from each participant.

The inclusion criteria were (1) newly developed active CNV confirmed with fundus fluorescein angiography (FFA), and (2) bilateral pathological myopia; defined as spherical equivalent of less than  $-6$  diopters (D) in phakic patients (unless previously undergone refractive surgery) or axial length more than 26.5 mm, with typical degenerative changes of pathological myopia.<sup>13</sup> Myopic CNV was defined as CNV associated with pathological myopic degenerative changes in the fundus. Patients with Fuch's hemorrhage or CNV secondary to other causes other than pathological myopia were excluded.

Eyes with mCNV were grouped under study group and fellow uninvolved eyes were used as comparison group.

### Clinical Examination

At baseline, all patients underwent standardized measurement of best corrected visual acuity (BCVA) using Snellen denominations, IOP, refractive error, and axial length using partial optical coherence interferometry (IOL Master; Carl Zeiss Meditec, Dublin, CA, USA). Snellen visual acuities were converted to logMAR equivalent for statistical analysis. The SD-OCT scan was performed using the Heidelberg Spectralis (Version 5.3.2.0; Heidelberg Engineering, Heidelberg, Germany). Fluorescein angiography was performed at presentation to confirm the presence of mCNV (TRC-50X/IMAGeNet 2000; Topcon, Tokyo, Japan; or Spectralis; Heidelberg Engineering, Heidelberg, Germany). The greatest linear dimension (GLD) of mCNV was measured based on angiographic images, using internal caliper software.

### Treatment and Follow-Up Schedule

All patients received treatment according to the standard of care and treatment was not altered by entering into the study. Generally all patients were reviewed monthly until mCNV was inactive, after which interval between monitoring visits was increased progressively. Patients were treated with either intravitreal bevacizumab (1.25 mg) or ranibizumab (0.50 mg) on the first visit and retreated on a pro-re-nata (PRN) protocol, based on results of randomized clinical trial results.<sup>8,9</sup> Decision for repeat treatment with anti-VEGF was made based on presence of persistent or recurrent subretinal, intraretinal fluid, or blood. All patients were reviewed at 6 months and 1 year during which BCVA and SD-OCT were repeated. Additional visits on an as needed basis were allowed.

### Measurement of Choroidal Thickness (CT)

Using the Heidelberg Spectralis, a volume scan of  $20^\circ \times 20^\circ$  containing at least 25 B-scans centering at the fovea, was obtained for each eye at baseline, 6, and 12 months. Individual B-scan was an average of nine frames and 240  $\mu\text{m}$  apart from the next B-scan. Baseline foveal horizontal section was used for the measurements of subfoveal CT (SFCT)<sup>4,7</sup> measured from the outer surface of the hyperreflective line ascribed to the RPE to the hyperreflective line of the inner sclera border. Nasal and temporal choroidal thickness were similarly measured at a distance 1500  $\mu\text{m}$  from the fovea. All measurements were performed by independent clinicians and the average of the two measurements were recorded and used for analysis. Where measurements differed by greater than 15%, a final measurement was agreed after open arbitration. Enhanced-depth imaging (EDI) was not used, but all eyes still showed this clear interface because of choroidal thinning.

### Image Binarization and CVI Calculation

We used the entire length of SD-OCT scan for binarization and length of all the scans used were similar. A modified approach of the protocol described by Sonoda et al.<sup>14</sup> and as described previously by our group was carried out.<sup>12,15-17</sup> The image was processed on public domain software Fiji<sup>18</sup> (Fig. 1A) Polygon tool was used to select the total choroid area (TCA), which was added in the region of interest (ROI) manager. After converting the image into 8 bit, Niblack auto local thresholding was subsequently applied that gives the mean pixel value with SD for all the points. The LA was highlighted by applying the color threshold and later added to the ROI manager. To determine the LA within the initially selected polygon, both the areas in ROI manager were selected and merged by AND operation. The composite third area was added to the ROI manager. The first area represents the total of the choroid selected, and the third composite area is the vascular or LA (Fig. 1B). The CVI was calculated by dividing LA by TCA and was calculated over the entire axial length of the scan irrespective if it was shorter or longer scans. Image grading was done by one of the authors who was a trained grader and was masked to the patients' information.

### Statistical Analysis

Statistical analyses were performed using SPSS version 22.0 (SPSS, Chicago, IL, USA). Distribution of normality was assessed using Shapiro-Wilk test. Mann-Whitney *U* test was used to assess the baseline difference of the spherical equivalent, axial length, visual acuity, CT, and CVI between fellow and mCNV eyes. Wilcoxon signed-rank test was used for comparisons between baseline, month 6, and month 12 for visual acuity, CT, and CVI. Myopic CNV eyes were further dichotomized into two groups - depending on presence of significant choroidal thinning. In view of generally thin choroidal layer in highly myopic eyes, percentage reduction instead of a fixed absolute reduction was regarded as a better assessment of the development of significant choroidal thinning. A difference in measurement of at least 15% in CT was considered significant.<sup>19</sup> Mann-Whitney *U* test,  $\chi^2$ , or Fisher's exact test were subsequently used to analyze associations of parameters with significant choroidal thinning in mCNV eyes. Significant factors were further analyzed using multivariate logistic regression analysis, adjusting for age, sex, axial length, spherical equivalent, number of intravitreal injections, baseline CT, as well as mCNV lesion location. Statistical significance was set at *P* less than 0.05 for all analysis.

### RESULTS

We included 20 patients with bilateral pathological myopia with unilateral mCNV, comparing mCNV eyes (study group) with fellow eyes without mCNV (control group). Baseline clinical data is presented in Table 1. The majority of the patients were women ( $n = 15$ ) and mean age was  $60.35 \pm 10.85$  years. The majority of mCNV were subfoveal or juxtafoveal in location. The mean GLD was  $716.42 \pm 739.75$   $\mu\text{m}$ . There were no differences in refractive error and axial length between mCNV group and contralateral eyes. As expected, BCVA at presentation was significantly worse in the mCNV group compared with contralateral eyes (logMAR  $0.65 \pm 0.67$  vs  $0.15 \pm 0.49$ ,  $P < 0.001$ ). The mean number of anti-VEGF injections received was  $2.20 \pm 1.01$  from baseline to month 12. Six patients received ranibizumab exclusively ( $1.50 \pm 0.50$  injections) and 14 patients received bevacizumab exclusively ( $2.50 \pm 1.00$  injections). Most of the treatments were given between baseline and month 6. Only two patients

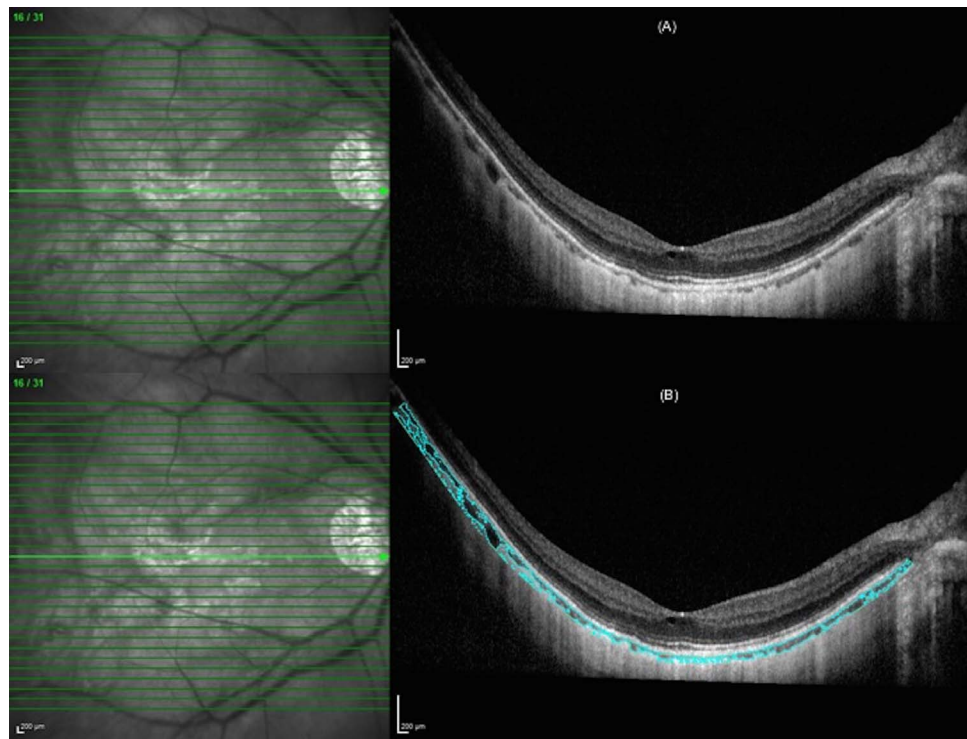


**FIGURE 1.** A single SD-OCT scan of a patient with myopic macular degeneration demonstrating dark pixelated areas (assumed as vascular or luminal areas - LA) and light pixelated areas (assumed as interstitial or stromal areas; *top photo [A]*). Image binarization was performed using Niblack auto local threshold on Fiji (public domain software). Postbinarization overlay of region of interest on the scan illustrating luminal (*dark pixelated region*) and stromal area (*light blue pixelated region; bottom photo [B]*).

received additional injections between month 6 and month 12. At baseline, there was no difference in CT in the three locations measured between mCNV group and contralateral eyes.

Longitudinal changes in BCVA, CT, and CVI at baseline, month 6 and month 12 are shown in Table 2. At month 12,

BCVA of mCNV group improved significantly to  $0.40 \pm 0.75$  ( $P = 0.013$ ). In the affected eyes, significant subfoveal choroidal thinning was noted at month 12 compared with baseline ( $54.75 \pm 45.43 \mu\text{m}$  vs.  $69.20 \pm 63.04 \mu\text{m}$ ,  $P = 0.017$ ). There was no significant difference in temporal and nasal CT at month 6 and 12 when compared against baseline. During the

**TABLE 1.** Baseline Demographics and Clinical Characteristics

Baseline Factor	mCNV, N = 20	Unaffected Eyes, N = 20	P*
Age, y	60.35 ± 10.85	60.35 ± 10.85	NA
Female, n (%)	15 (75.0)	15 (75.0)	NA
Chinese, n (%)	20 (100.0)	20 (100.0)	NA
Duration of symptoms before treatment, mo	4.31 ± 13.22	4.31 ± 13.22	NA
Spherical equivalent, D	-10.90 ± 3.63	-11.35 ± 5.83	0.929
Axial length, mm	28.82 ± 1.31	28.72 ± 2.16	0.885
FFA lesion size, $\mu\text{m}$	716.42 ± 739.75	-	NA
Location on FFA			
Subfoveal, n (%)	9 (45.0%)	-	NA
Juxtafoveal, n (%)	5 (25.0%)	-	NA
Extrafoveal, n (%)	6 (30.0%)	-	NA
Intravitreal injections	2.20 ± 1.01	-	NA
Baseline			
Visual acuity, logMAR	0.65 ± 0.67	0.15 ± 0.49	<b>&lt;0.001</b>
Choroidal thickness, $\mu\text{m}$			
Subfoveal	69.20 ± 63.04	67.10 ± 65.74	0.713
Nasal	79.15 ± 68.06	85.80 ± 54.95	0.473
Temporal	103.95 ± 68.53	104.30 ± 76.79	0.878
CVI, %	59.44 ± 3.92	59.03 ± 5.58	0.958

\* P value comparing eyes with mCNV with fellow unaffected eyes at baseline using Mann-Whitney U test. Bold indicates significant P value. NA, not applicable.

**TABLE 2.** Comparison of Visual Acuity, Choroidal Thickness (Subfoveal, 1500- $\mu$ m Nasal, and Temporal to Center of Fovea), and Choroidal Vasculature Index Between Baseline, Month 6 and Month 12

Ocular Feature	mCNV, N = 20	P Value*	Unaffected Eyes, N = 20	P Value*
<b>Visual acuity</b>				
Baseline, logMAR	0.65 $\pm$ 0.67	Ref	0.15 $\pm$ 0.49	Ref
Month 6, logMAR	0.56 $\pm$ 0.63	0.06	0.28 $\pm$ 0.32	0.85
Month 12, logMAR	0.40 $\pm$ 0.75	<b>0.013</b>	0.15 $\pm$ 0.49	0.564
<b>Choroidal thickness</b>				
<b>Subfoveal</b>				
Baseline, $\mu$ m	69.20 $\pm$ 63.04	Ref	67.10 $\pm$ 65.74	Ref
Month 6, $\mu$ m	59.69 $\pm$ 61.32	0.21	60.38 $\pm$ 72.55	0.109
Month 12, $\mu$ m	54.75 $\pm$ 45.43	<b>0.017</b>	67.10 $\pm$ 64.00	0.657
<b>Nasal</b>				
Baseline, $\mu$ m	79.15 $\pm$ 68.06	Ref	85.80 $\pm$ 54.95	Ref
Month 6, $\mu$ m	66.69 $\pm$ 66.90	0.075	81.94 $\pm$ 69.62	0.967
Month 12, $\mu$ m	77.79 $\pm$ 62.02	0.534	81.16 $\pm$ 60.77	0.907
<b>Temporal</b>				
Baseline, $\mu$ m	103.95 $\pm$ 68.53	Ref	104.30 $\pm$ 76.79	Ref
Month 6, $\mu$ m	94.00 $\pm$ 65.16	0.368	94.94 $\pm$ 80.31	0.113
Month 12, $\mu$ m	101.53 $\pm$ 63.92	0.961	100.42 $\pm$ 73.29	0.384
<b>CVI</b>				
Baseline, %	59.44 $\pm$ 3.92	Ref	59.03 $\pm$ 5.58	Ref
Month 6, %	58.59 $\pm$ 4.04	0.635	59.27 $\pm$ 5.75	0.81
Month 12, %	59.25 $\pm$ 5.28	0.98	59.67 $\pm$ 7.46	0.548

\* P value comparing against baseline using Wilcoxon Signed Ranks test. Bold indicates significant P value. Ref, reference.

same period, no significant change in CVI was observed. There were no significant changes in the contralateral eyes for BCVA, CT, and CVI over 12 months. Figure 2 illustrates the changes in CT in treated eyes at baseline, month 6, and month 12.

We further evaluated the influence of baseline risk factors and treatment exposure on the likelihood of eyes developing significant thinning (defined as  $\geq 15\%$  from baseline) of SFCT (Table 3). Out of 20 eyes in the mCNV group, 11 (55.0%) developed significant SFCT at 12 months. In the univariate analysis, thicker baseline SFCT ( $89.27 \pm 75.70 \mu\text{m}$  vs.  $44.67 \pm 32.32$ ,  $P = 0.016$ ) and extrafoveal location of the CNV ( $54.5\%$  vs.  $0.0\%$ ,  $P = 0.023$ ) were associated with significant subfoveal choroidal thinning over time. However, after adjusting for multiple factors, none of the factors were significant. Final BCVA at month 12 between study eyes with and without significant SFCT thinning were not significantly different.

## DISCUSSION

Alterations in the choroidal circulation may contribute toward degenerative changes in pathological myopia and highly myopic eyes.<sup>19</sup> Narrowing and loss of large choroidal vessels, and occlusion of choriocapillaris have been suggested to be important in the pathogenesis of chorioretinal atrophy in pathological myopia.<sup>4</sup> Vascular changes and ischemia have also been proposed to be important factors in the pathogenesis of lacquer cracks and myopic CNV.<sup>3,20,21</sup> These theories have subsequently been supported to a certain extent by demonstration of associations between choroidal thinning, measured on OCT, with lacquer cracks and mCNV, independent of axial length or refractive error.<sup>4,6,10,19,22</sup> However, there have been no studies evaluating choroidal vascularity in mCNV. The CVI is a novel tool to quantitatively describe the choroidal vasculature, and is calculated as the proportion of LA to TCA. The CVI

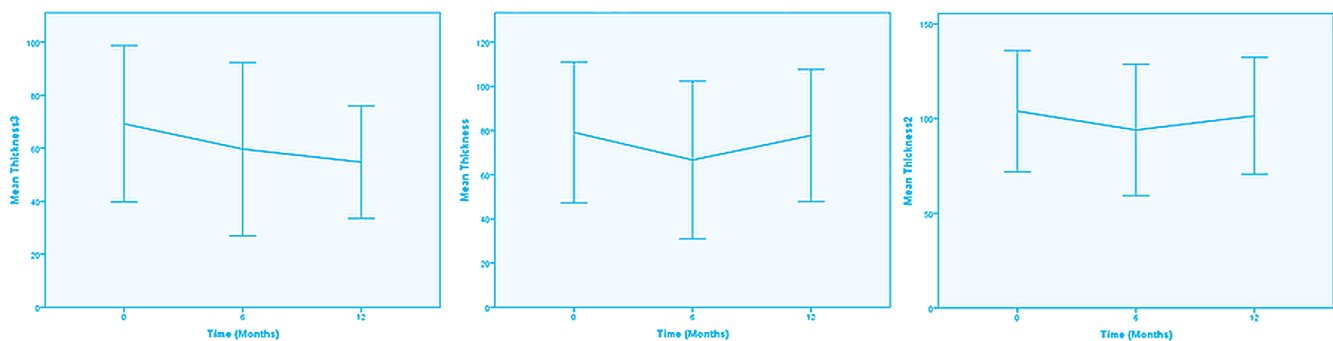


**FIGURE 2.** Line graph depicting the temporal variation in subfoveal (*left*), nasal (*middle*), and temporal choroidal (*right*) thickness in eyes with myopic CNV. A gradual decline in subfoveal choroidal thickness was observed over 12 months, which was not present in both nasal and temporal choroids.

TABLE 3. Comparison of Risk Factors Between Eyes With and Without Significant Subfoveal Choroidal Thinning Over 12 Months

Risk Factor	Significant Thinning of Subfoveal Choroid* (N = 11)	No Significant Thinning of Subfoveal Choroid (N = 9)	P†	P‡
Age, y	59.55 ± 9.63	61.33 ± 12.72	0.752	-
Female, n (%)	8 (72.73)	7 (77.78)	0.604	-
Axial length, mm	28.76 ± 1.59	28.89 ± 1.00	0.661	-
Spherical equivalent, D	-10.80 ± 4.34	-11.01 ± 2.41	0.714	-
Location				
Subfoveal, n (%)	4 (36.40)	5 (55.60)	<b>0.023</b>	0.997
Juxtafoveal, n (%)	1 (9.10)	4 (44.40)	-	-
Extrafoveal, n (%)	6 (54.50)	0 (0.00)	-	-
FFA lesion size, μm	631.66 ± 767.98	811.78 ± 740.48	0.661	-
Total injections	2.36 ± 0.92	2.00 ± 1.12	0.447	-
Baseline visual acuity, logMAR	0.67 ± 0.38	0.80 ± 0.72	0.619	-
Baseline subfoveal choroidal thickness, μm	89.27 ± 75.70	44.67 ± 32.32	<b>0.016</b>	0.999
Baseline CVI, %	60.11 ± 3.54	58.52 ± 4.46	0.454	-
Month 12 visual acuity (LogMAR)	0.46 ± 0.56	0.60 ± 0.81	0.823	-

Bold indicates significant *P* value.

\* Significant thinning defined as decrease by at least 15% from baseline SFCT.

† *P* value analyses using Mann-Whitney *U* test and  $\chi^2$  or Fisher's exact test for continuous and categorical variables, respectively.

‡ *P* value obtained using logistic regression analysis. Risk factors were adjusted for age, sex, spherical equivalent, axial length, number of intravitreal injections, baseline SFCT, and lesion location.

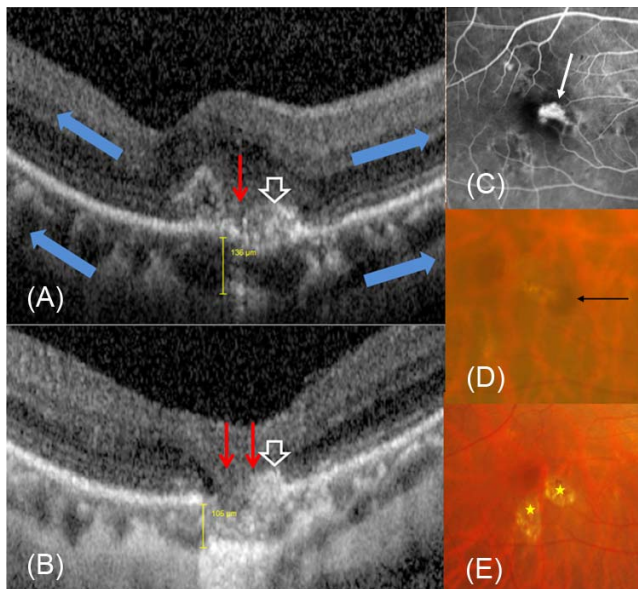


FIGURE 3. (A–E) Female (59-years old) with right mCNV. (A) Spectral-domain OCT at baseline with a subfoveal choroidal thickness (SFCT) of 136 μm measured with built-in caliper. The red arrow marks the site of Bruch membrane (BM) break. White hollow arrow identifies the mCNV adjacent to the BM break. Blue block arrows demonstrate the direction of the centrifugal force exerted on the neurosensory retina, RPE, and choroid. (B) Spectral-domain OCT at month 12 with a significantly thinner SFCT under the area of BM break (106 μm). Note the extension of the BM break, demarcated at the edges by the red arrows, in comparison to baseline. The adjacent mCNV has consolidated and reduced in size (white hollow arrow). Hypertransmission within the corresponding area of chorioretinal atrophy (CRA) can be seen. (C) Venous phase of the fundus fluorescein angiogram showing a well-defined subfoveal area of hyperintensity with leakage corresponding to the location of the mCNV (white arrow). (D) Color photograph at baseline with an area of subretinal hemorrhage overlying the mCNV (black arrow). (E) Color photograph at month 12 highlighting the development of CRA (yellow star), corresponding with findings on Figure 3B.

is an indirect measure of choroidal vascularity. In our current study, we demonstrated thinner baseline SFCT in both study eyes with mCNV and fellow control eyes in patients with bilateral pathological myopia. Subfoveal CT in the mCNV eyes decreased significantly from baseline to month 12 with anti-VEGF treatment, but did not change in the contralateral eyes without mCNV. Importantly, we showed that the reduction in SFCT was not accompanied by temporal change in CVI, indicating that there is generalized thinning in both stromal and vascular components.

Progressive choroidal thinning has been reported in eyes with neovascular AMD treated with anti-VEGF.<sup>23</sup> In particular, because VEGF plays an important physiological role in the maintenance of choroidal vascular health and function, the possibility of long-term anti-VEGF therapy leading to atrophy on the choroid and RPE remain a concern.<sup>24,25</sup> Because highly myopic eyes and eyes with pathological myopia commonly have thin choroid, the concern for progressive choroidal thinning is even greater in eyes with mCNV receiving anti-VEGF therapy. As the choroid plays a crucial role in supporting photoreceptor function, such thinning may have significant deleterious impact on outer retina and RPE health. Our results showed that SFCT did decline significantly in eyes with mCNV 12 months after initiation of anti-VEGF therapy. However, this choroidal thinning was not associated with worse final BCVA. Similar findings have also been reported in a recent study in Korean patients.<sup>10</sup> We also did not find any association between number of anti-VEGF injections and the risk of developing significant choroidal thinning. While this is reassuring for the shorter-term safety of anti-VEGF therapy for mCNV, clearly, longer-term follow-up of changes in CT, CVI, and visual outcomes are necessary.

To our best knowledge, we are the first group to investigate the possible underlying mechanism for the reduction in SFCT by studying changes in the luminal and stromal area within the choroid on OCT. The CVI is a novel tool to quantitatively describe the choroidal vasculature, and we have previously established normative database of CVI from a large study involving 345 subjects and estimated the average CVI in healthy eyes to be  $65.61 \pm 2.33\%$ .<sup>12</sup> In a separate study of 42

eyes with exudative AMD, we found a reduction in baseline CVI (mean CVI 60.14%; manuscript in revision, 2016). In the current study, we report that in this series of eyes with pathological myopia, even lower CVI was noted in both mCNV eyes and contralateral eyes (mean CVI 59.44% and 59.03%, respectively). Over a 12-month follow-up period, we found that CVI remained unchanged, despite progressive reduction of SFCT in the mCNV eyes. We had expected a priori that the reduction in SFCT was predominantly a reflection of reduction in vasculature within the choroid. However, the finding of preserved CVI suggests that there is generalized loss in both vascular and stromal area.

Recently, Ohno-Matsui et al.<sup>26</sup> reported that up to 76% of eyes with mCNV-related macular atrophy showed macular Bruch membrane defects. These defects may enlarge as a result of axial expansion of the eye.<sup>26,27</sup> We hypothesize with progressive globe elongation, the bridging tissues on either side of the Bruch membrane hole, namely RPE and choroid, will be subjected to centrifugal expansive forces (Figures 3A-E). This results in mechanical stretching of the choroid, which in turn can lead to thinning of both stromal and vascular components. Therefore CVI remained unchanged while SFCT became progressively reduced. In contrast, if choroidal thinning was due to ischemia, one would expect to see preferential loss of vascular/luminal area and reduced CVI in tandem with reduction in SFCT. Our findings do not support this latter theory.

There are several limitations to our study that needs to be considered. Firstly, our study has a small sample size with low injection episodes. Secondly, EDI was not available when the patients were recruited for this study. However, all SD-OCT images used for measurements were able to demonstrate a clear interface between the choroid and the sclera as a result of generalized choroidal thinning in highly myopic eyes. Thirdly, differences in CT would be easier to detect and measure manually with the in-built caliper software when the baseline CT is larger, which could account for the observation of more significant thinning in eyes with thicker baseline SFCT. The choice of 15% thinning as significant thinning was arbitrary but has been used in previous study.<sup>19</sup>

In conclusion, we report that thinning of subfoveal choroidal, but not choroidal vascularity, as measured using the CVI, was observed in eyes with mCNV treated with anti-VEGF over 12 months. Choroidal thinning did not influence final BCVA over the 12 months. Our findings thus suggest that changes in CT with treatment may be via structural factors (e.g., mechanical stretching in response to globe expansion) rather than vascular factors.

### Acknowledgments

Supported by a SingHealth Foundation Grant SHF/FG389S/2009 (Singapore).

Disclosure: **W.Y. Ng**, None; **D.S.W. Ting**, None; **R. Agrawal**, None; **N. Khandelwal**, None; **H.M. Htoon**, None; **S.Y. Lee**, None; **T.Y. Wong**, None; **G.C.M. Cheung**, None

### References

- Cohen SY, Laroche A, Leguen Y, Soubrane G, Coscas GJ. Etiology of choroidal neovascularization in young patients. *Ophthalmology*. 1996;103:1241-1244.
- Wong TY, Ferreira A, Hughes R, Carter G, Mitchell P. Epidemiology and disease burden of pathologic myopia and myopic choroidal neovascularization: an evidence-based systematic review. *Am J Ophthalmol*. 2014;157:9-25, e12.
- Neelam K, Cheung CM, Ohno-Matsui K, Lai TY, Wong TY. Choroidal neovascularization in pathological myopia. *Prog Retin Eye Res*. 2012;31:495-525.
- Fujiwara T, Imamura Y, Margolis R, Slakter JS, Spaide RF. Enhanced depth imaging optical coherence tomography of the choroid in highly myopic eyes. *Am J Ophthalmol*. 2009;148:445-450.
- Grossniklaus HE, Green WR. Pathologic findings in pathologic myopia. *Retina*. 1992;12:127-133.
- Flores-Moreno I, Lugo F, Duker JS, Ruiz-Moreno JM. The relationship between axial length and choroidal thickness in eyes with high myopia. *Am J Ophthalmol*. 2013;155:314-319, e311.
- Cheung CM, Loh BK, Li X, et al. Choroidal thickness and risk characteristics of eyes with myopic choroidal neovascularization. *Acta Ophthalmol*. 2013;91:e580-e581.
- Wolf S, Balciuniene VJ, Laganovska G, et al. RADIANCE: a randomized controlled study of ranibizumab in patients with choroidal neovascularization secondary to pathologic myopia. *Ophthalmology*. 2014;121:682-692, e682.
- Ikuno Y, Ohno-Matsui K, Wong TY, et al. Intravitreal aflibercept injection in patients with myopic choroidal neovascularization: the MYRROR Study. *Ophthalmology*. 2015;122:1220-1227.
- Ahn SJ, Park KH, Woo SJ. Subfoveal choroidal thickness changes following anti-vascular endothelial growth factor therapy in myopic choroidal neovascularization. *Invest Ophthalmol Vis Sci*. 2015;56:5794-5800.
- Farinha CL, Baltar AS, Nunes SG, et al. Choroidal thickness after treatment for myopic choroidal neovascularization. *Eur J Ophthalmol*. 2013;23:887-898.
- Agrawal R, Gupta P, Tan KA, Cheung CM, Wong TY, Cheng CY. Choroidal vascularity index as a measure of vascular status of the choroid: measurements in healthy eyes from a population-based study. *Sci Rep*. 2016;6:21090.
- Ohno-Matsui K, Kawasaki R, Jonas JB, et al. International photographic classification and grading system for myopic maculopathy. *Am J Ophthalmol*. 2015;159:877-883, e877.
- Sonoda S, Sakamoto T, Yamashita T, et al. Choroidal structure in normal eyes and after photodynamic therapy determined by binarization of optical coherence tomographic images. *Invest Ophthalmol Vis Sci*. 2014;55:3893-3899.
- Tan KA, Laude A, Yip V, Loo E, Wong EP, Agrawal R. Choroidal vascularity index - a novel optical coherence tomography parameter for disease monitoring in diabetes mellitus [published online ahead of print May 6, 2016]. *Acta Ophthalmol*. doi: 10.1111/aos.13044.
- Agrawal R, Chhablani J, Tan KA, Shah S, Sarvaiya C, Banker A. Choroidal vascularity index in central serous chorioretinopathy. *Retina*. 2016;36:1646-1651.
- Agrawal R, Salman M, Tan KA, et al. Choroidal vascularity index (CVI) - a novel optical coherence tomography parameter for monitoring patients with panuveitis? *PLoS One*. 2016;11:e0146344.
- Schindelin J, Arganda-Carreras I, Frise E, et al. Fiji: an open-source platform for biological-image analysis. *Nat Methods*. 2012;9:676-682.
- Nishida Y, Fujiwara T, Imamura Y, Lima LH, Kurosaka D, Spaide RF. Choroidal thickness and visual acuity in highly myopic eyes. *Retina*. 2012;32:1229-1236.
- Wakabayashi T, Ikuno Y. Choroidal filling delay in choroidal neovascularization due to pathological myopia. *Br J Ophthalmol*. 2010;94:611-615.
- Wong TY, Ohno-Matsui K, Leveziel N, et al. Myopic choroidal neovascularisation: current concepts and update on clinical management. *Br J Ophthalmol*. 2015;99:289-296.

22. Wang NK, Lai CC, Chou CL, et al. Choroidal thickness and biometric markers for the screening of lacquer cracks in patients with high myopia. *PLoS One*. 2013;8:e53660.
23. Ting DS, Ng WY, Ng SR, et al. Choroidal thickness changes in age-related macular degeneration and polypoidal choroidal vasculopathy: a 12-month prospective study. *Am J Ophthalmol*. 2016;164:128-136, e1.
24. Saint-Geniez M, Maldonado AE, D'Amore PA. VEGF expression and receptor activation in the choroid during development and in the adult. *Invest Ophthalmol Vis Sci*. 2006;47:3135-3142.
25. Maharaj AS, Saint-Geniez M, Maldonado AE, D'Amore PA. Vascular endothelial growth factor localization in the adult. *Am J Pathol*. 2006;168:639-648.
26. Ohno-Matsui K, Jonas JB, Spaide RF. Macular Bruch membrane holes in choroidal neovascularization-related myopic macular atrophy by swept-source optical coherence tomography. *Am J Ophthalmol*. 2016;162:133-139, e131.
27. Hayashi K, Shimada N, Moriyama M, Hayashi W, Tokoro T, Ohno-Matsui K. Two-year outcomes of intravitreal bevacizumab for choroidal neovascularization in Japanese patients with pathologic myopia. *Retina*. 2012;32:687-695.